Cancellation of Fabry-Perot interference effects in terahertz time-domain spectroscopy of optically thin samples

Renato Fastampa,[1,2,*] Laura Pilozzi,[3] and Mauro Missori[2]

[1]*Dipartimento di Fisica, Università di Roma "Sapienza", Piazzale Aldo Moro 5, 00185 Roma, Italy*

[2]*Istituto dei Sistemi Complessi, Consiglio Nazionale delle Ricerche, Unità Sapienza, Piazzale Aldo Moro 5, 00185 Roma, Italy*

[3]*Istituto dei Sistemi Complessi, Consiglio Nazionale delle Ricerche, Via dei Taurini 19, 00185 Roma, Italy*

(Received 5 April 2017; published 20 June 2017)

Terahertz time-domain spectroscopy is increasingly used in many fields of research. For strongly absorbing materials with refraction index close to 1, optical parameters at terahertz frequencies are most conveniently quantified using transmission measurements through thin samples. Unfortunately, extracting optical parameters from raw data implies the use and/or development of complicated numerical data processing procedures. In this work we present an efficient computational procedure for extracting the optical parameters in very thin samples ($\lesssim$100 μm) from transmission terahertz time-domain spectroscopy. In our procedure, we are able to successfully remove from raw data the Fabry-Perot interference effects, which are commonly recognized to be the leading cause of inaccuracy in the extracted parameters, introducing fictitious oscillations in their frequency dependence. The procedure is based on the Davidenko method to identify the roots of complex functions used to numerically solve the implicit equation obtained by equating the experimental and theoretical transfer functions. The advantage of the method is the possibility of obtaining the roots using the numerical solution of a system of real differential equations using standard mathematical packages. In addition, we show that complete removal of the Fabry-Perot oscillations is achieved by including in the computational procedure, besides the sample thickness, the instrumental error on the starting instant of the terahertz signal sampling. This error could be common to many terahertz time-domain systems, especially those using optical fibers. This correction is necessary in general to preserve the terahertz spectroscopic features in the extracted optical parameters for strongly absorbing materials with refraction index close to 1, such as water, biological matter, and several organic materials.

DOI: 10.1103/PhysRevA.95.063831

I. INTRODUCTION

In recent years, technological advances in the generation of coherent sources have made terahertz (THz) time-domain spectroscopy (TDS) [1] available to an ever wider audience of researchers working in different fields. This technique is based on the emission of THz pulses with a duration in the range of picoseconds. Many sources of THz radiation have been proposed so far: photoconductive antennae, collinear optical rectification in electro-optic materials, tilted pulse generation in $LiNbO_3$, rectification in organic crystals, and mixed-field air plasma [1]. Photoconductive antennae are semiconductor structures with a short carrier lifetime. Terahertz pulses are generated switching the antenna using an ultrafast laser pulse with a duration of some tens of femtoseconds, thus causing the applied bias to generate a rapidly varying photocurrent. Detection of the THz pulse is realized by another photoconductive antenna, which works as a dipole when excited by the ultrafast laser pulse. This causes the incoming THz pulse to induce a small current as the output signal. By using an optical delay line, the beam path difference between the THz path and the detector antenna laser path can be varied and used to sample the THz electrical field at the detector antenna $E(t)$ as a function of time (stroboscopic sampling) [2,3].

Transmission and reflection spectroscopy can be used for the measurement of the complex refractive index of a sample versus frequency ω, $\hat{n}(\omega) = n(\omega) + i\alpha(\omega)c/2\omega$, where $\alpha(\omega)$ is the absorption coefficient, $n(\omega)$ is the phase refraction index, and c is the speed of light. In the simplest transmission experiment, two time-domain THz pulses $E(t)$, propagating through the sample and through vacuum or air, respectively, are recorded and their calculated spectral amplitude and phase $\hat{E}_{\text{sample}}(\omega)$ and $\hat{E}_{\text{ref}}(\omega)$ are compared by using the complex transfer function $\hat{T}(\omega)$ defined as

$$\hat{T}(\omega) = T(\omega)e^{i\varphi(\omega)} = \frac{\hat{E}_{\text{sample}}(\omega)}{\hat{E}_{\text{ref}}(\omega)}, \tag{1}$$

where $\varphi(\omega)$ is the transfer function phase [3]. The variation in frequency of $\hat{n}(\omega)$ can be obtained by solving the inverse scattering problem for the electromagnetic waves, namely, by equating the experimental transfer function

$$\hat{T}_{\text{expt}}(\omega_j) = \frac{\hat{E}_{\text{sample}}(\omega_j)}{\hat{E}_{\text{ref}}(\omega_j)}$$

(j is a data array index) with the analytical expression of $\hat{T}(\hat{n},\omega_j)$ obtained by solving the direct electromagnetic problem.

However, the coherence of the THz radiation in THz TDS represents a critical issue for the extraction of the optical parameters from data due to interference effects caused by multiple reflections within the sample. In fact, when the THz pulse propagates within a sample, it will undergo internal reflections whenever an interface is encountered, transmitting at the same time part of the incident radiation. Multiple reflections at the interfaces generate echoes following the main THz pulse in the $E(t)$ signal. These interference effects will in general result in a complicated response of the sample to the electromagnetic stimulus, depending on $\hat{n}(\omega)$ as well as

*renato.fastampa@roma1.infn.it

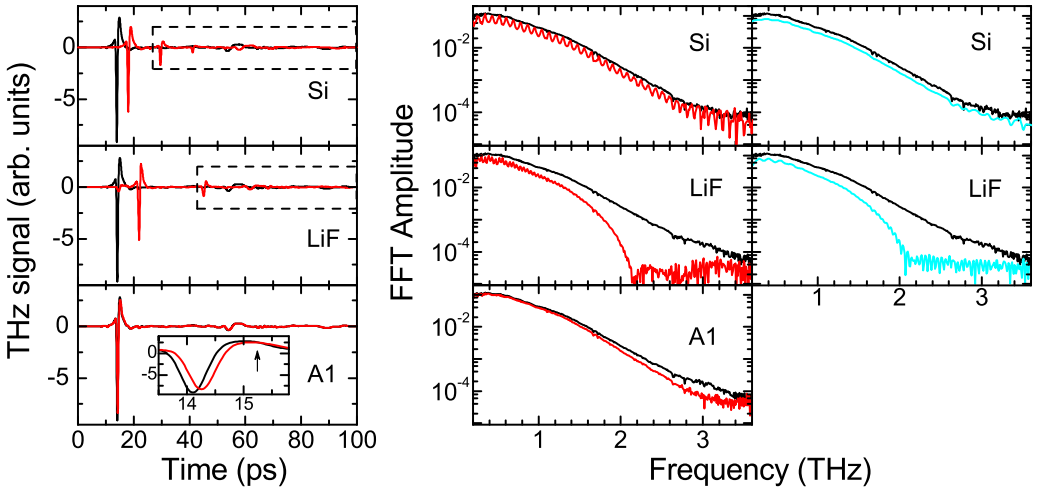

FIG. 1. Shown on the left are time traces of the reference (black line) and sample [red (gray) line] pulses from the transmission THz TDS experiments for all three samples. The inset shows that the first echo peak for the thinner sample A1 is expected to be superimposed on the main peak (indicated by the arrow) but is not evident. On the right is the FFT amplitude as obtained from the FFT of the full [red (gray) line] and truncated [cyan (light gray) line] time trace data of the left panel. The dashed-line rectangles delimit the truncated range of the Si and LiF time traces.

on the shape of the sample itself. In fact, in properly designed systems, this dependence can be exploited to control wave propagation so that response is governed by geometry as opposed to composition [4].

Therefore, one of the problems that must be addressed using THz TDS is the disentanglement of the optical parameters from the interference effects in the solution of the inverse scattering problem for the electromagnetic waves. A considerable simplification is obtained by using radiation incident perpendicularly on the flat surface of a homogeneous rectangular sample. This simplification is acceptable if the interface roughness is smaller than the probe radiation wavelength.

In a standard geometry in which the radiation impinges, from vacuum or air, perpendicularly on a flat sample, multiple reflections inside the sample give rise to the well-known Fabry-Perot (FP) interference effect. In this case the analytical expression of $\hat{T}(\hat{n},\omega)$, obtained trough the transfer matrix method [5], is

$$\hat{T}(\hat{n},\omega) = \frac{4\hat{n}}{(1+\hat{n})^2} \frac{e^{i(\hat{n}-1)\omega d/c}}{1-\left(\frac{\hat{n}-1}{\hat{n}+1}\right)^2 e^{2i(\omega/c)\hat{n}d}}, \qquad (2)$$

where d is the sample thickness and the denominator of the second factor represents the FP contribution. Extraction of the optical parameters can be obtained by equating theoretical and experimental transfer function: $\hat{T}(\hat{n},\omega_j) = \hat{T}_{\text{expt}}(\omega_j)$. However, this expression cannot be analytically inverted in order to express the optical parameters in terms of the experimental quantities.

Nevertheless, for optically thick samples, a simplified procedure, which will be described in detail in Sec. III, is possible. In these cases the main sample THz pulse is well separated in time from the echoes. This allows the sample and reference $E(t)$ signals to be truncated before the appearance of the first echo, avoiding the FP interference effects in $\hat{T}_{\text{expt}}(\omega_j)$ [see the red (full time trace) and blue (truncated) curves of the fast Fourier transform (FFT) amplitude in Fig. 1]. Finally, the FFT of the truncated curves allows the use of the analytically invertible Eq. (3) instead of Eq. (2).

Thin samples will instead lead to a sequence of echoes following closely or being superimposed on the main THz pulse and making the truncation procedure very difficult, if not impossible. In this case the FFT amplitude shows almost imperceptible slowly varying FP oscillations in the $\hat{T}_{\text{expt}}(\omega_j)$ (see the red curve A1 of the FFT amplitude in Fig. 1). Despite the apparently small amplitude of these oscillations, use of Eq. (3) gives rise to fictitious oscillations in the extracted optical parameters that can distort real spectroscopic features (see the black curves A1 in Fig. 2). In general, it is then necessary to use numerical algorithms to extract the optical parameters from the THz TDS measurements using Eq. (2). Several authors in the past have proposed different numerical methods to perform accurate cancellation of FP oscillations in thin samples. All of them had shown that such cancellation depends critically on the thickness parameter and proposed

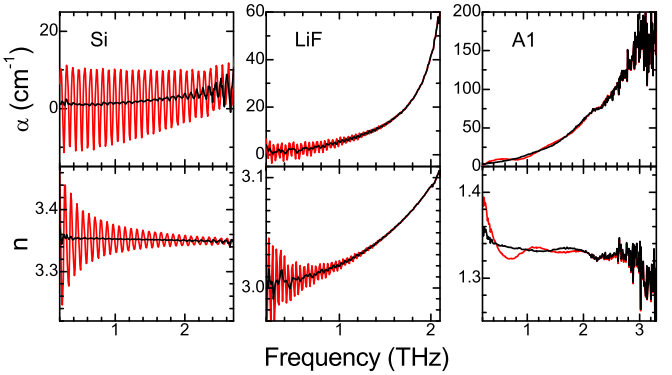

FIG. 2. Absorption coefficient and refraction index as a function of frequency as obtained by Eqs. (4) and (5) (black line) and after FP cancellation [red (gray) line] for all three samples.

some criteria in order to establish the best value at which this cancellation is optimal [6–11].

In this paper we present a computational procedure for extracting optical parameters from THz TDS measurements, able to provide the optical parameters of thin samples ($\lesssim$100 μm) with refraction index close to 1. This algorithm, different from previous methods, is based on the Davidenko method for finding the roots of complex functions. This method has already been used in the past to solve electromagnetic problems in multilayer dielectric structures. Compared to other methods, it has the advantage that the initial values, necessary for the numerical solution, do not need to be very close to the true solution as in the widely used Newton-Raphson (NR) method [6,12].

Furthermore, the proposed algorithm incorporates in a simple and computationally efficient way the correction of the temporal drift of the starting time of the stroboscopic sampling, affecting the sample-reference delay time. This correction allows the accurate extraction of the optical parameters for samples of thickness $\lesssim$100 μm and refraction index close to 1, up to now based on the adjustment of the thickness parameter only. This inaccuracy is likely present in many THz TDS setups, in particular in those based on optical fiber transmission of the laser pulse to the antennae. Its correction should be considered whenever the THz pulse delay time between reference and sample is comparable to this inaccuracy.

II. EXPERIMENT

A. Materials

In order to show the functioning of our computational method in significantly different situations, we selected three samples: a Si crystal (named Si), a LiF crystal (named LiF), and a specimen (named A1) from an ancient paper sheet. The sample Si is square shaped with an edge of 2 cm and is obtained from a B-doped polished silicon wafer with a resistivity of 100 Ω cm. The LiF sample is a polished, nominally pure, LiF crystal square shaped with a side of 1.5 cm, containing point defects (color centers) induced by γ radiation [13,14]. The sample A1 is a piece of about 2×4 cm^2 of unprinted paper produced in 1413 in Perpignan (France) and made from cotton and linen cellulose, already used for several studies [15–19]. The samples may be considered as representative of as many paradigmatic classes of solid materials at the THz frequencies: Si is low absorbent, high refractive index; LiF is medium absorbent, high refractive index; and A1 is strong absorbent, low refractive index and very thin. All samples are shaped according to the standard geometry used for transmission mode measurements and are considered to meet the general assumption of facing two flat and parallel surfaces perpendicular to the direction of propagation. Scattering for the porous sample A1 can be neglected as the length scale of inhomogeneities (of the order of tens of micrometers) is smaller than the THz wavelength [20,21]. In Table I main sample data and information are reported.

As widely noted in previous works [8,10,11], the values of the sample thickness used in a numerical extraction method have to be adjusted to achieve the complete cancellation of the FP oscillation from the optical parameters. In fact, the precision necessary in the thickness measurement in this case is higher than that obtainable by a micrometer screw gauge. Then the thickness t reported for A1 represents only the initial value used in our algorithm but not the value that gives the best FP cancellation (d values). For the other two samples the presence of the echoes is exploited for a more precise determination (d^* values), but a slight adjustment is necessary for LiF.

TABLE I. Sample thickness, measured by a micrometer, t; estimated by Eq. (6), d^*; and best value from the numerical procedure, d. Also reported are the refraction index n and absorption coefficient α at $\sim$1.5 THz.

Name	$t \pm 0.01$ (mm)	d^* (mm)	d (mm)	n	α (cm^{-1})
Si	0.52	0.519	0.519	3.35	$\approx$1
LiF	1.15	1.138	1.154	3.05	$\approx$10
A1	0.108		0.115	1.35	$\approx$25

B. Method

Terahertz spectra were recorded in transmission mode using a Menlo Systems (Germany) TERA K15 THz TDS equipped with photoconductive antennae excited by a femtosecond fiber-coupled laser (Menlo Systems T-Light). The laser emission wavelength was 1560 nm, the repetition frequency 100 MHz, and the pulse duration approximately 90 fs. For all acquisitions the delay line scan range was 100 ps, the scan rate was 8 Hz, and data were pitched every 33 fs. Spectra were obtained by averaging the signal over 400 scans (each lasting 0.125 s), therefore the time for a single acquisition was 50 s.

Since water vapor absorbs THz radiation, prior to spectra acquisition, the sample compartment of the THz setup was purged with N_2 until most water vapor absorption lines were indistinguishable from noise (nearly 60 min). The usable range for this apparatus was found to be 0.2–3.5 THz. The frequency-dependent dynamic range obtained by averaging over 400 scans was about 77 dB at 0.35 THz and about 20 at 3.5 THz.

Terahertz radiation emitted by the photoconductive antenna was collected and focused to the sample by means of two TPX lenses with 50-mm nominal focal length. Radiation transmitted through the sample was collected and focalized to the receiver antenna by another pair of identical 50-mm nominal focal length TPX lenses. All samples were placed in the transmission lines with the two flat parallel surfaces orthogonal to the THz beam line axis.

C. Terahertz data analysis

Typical THz pulses propagating without the sample (reference signal) and through the sample are shown in Fig. 1 for Si, LiF, and A1 (left panels). The presence of multiple echoes following the main THz pulse is well evident for Si and LiF samples. The blue dashed line in the rectangles in the left panel delimit the truncated range of the Si and LiF time traces.

Terahertz pulse data arrays were converted in spectral data by a standard discrete FFT algorithm. The resulting curves for the full (red) and truncated (blue) time traces are shown in the

right panels of Fig. 1. The presence of multiple pulse echoes in the time trace introduces oscillations in the FFT [7]. Such oscillations are evident in the sample FFT amplitude for Si, less evident for LiF, and apparently absent for A1.

III. COMPUTATIONAL METHOD

As explained in the Introduction, the extraction of $\hat{n}(\omega)$ from the THz TDS signal measured in transmission mode can be carried out by using $\hat{T}(\hat{n},\omega)$ [Eq. (1)]. Equating the experimental transfer function $\hat{T}_{\text{expt}}(\omega_j)$ with $\hat{T}(\hat{n},\omega_j)$ obtained by solving the direct electromagnetic problem (2) allows the recovery of $\hat{n}(\omega)$.

The solution of this equation requires a numerical approach. On the contrary, a simpler approach can be used in the special case of optically thick samples or whenever the echo peaks are well separated in the sample time trace. In this case, it is possible to truncate the pulse data array before the appearance of the echoes (see Fig. 1) and use as a theoretical transfer function the expression

$$\hat{T}(\hat{n},\omega) = \frac{4\hat{n}}{(1+\hat{n})^2} e^{-\alpha d/2} e^{i(n-1)\omega d/c} \tag{3}$$

in which the multiple reflections are neglected [7].

Equation (3) can be easily inverted when equated to the experimental transfer function if the absorption contribution in the first factor of the equation is first neglected, obtaining

$$n(\omega) = 1 + \frac{\varphi_{\text{expt}}(\omega)c}{\omega d}, \tag{4}$$

$$\alpha(\omega) = -\frac{2}{d}\ln\left(\frac{(1+n)^2}{4n} T_{\text{expt}}(\omega)\right) \tag{5}$$

Here care must be taken in the numerical procedure used to unwrap the experimental phase $\varphi_{\text{expt}}(\omega_j)$ that can introduce fictitious sudden phase jumps of 2π [8].

As already evidenced in many previous works, regardless of the transfer function used, the extracted values of $\hat{n}(\omega)$ depend critically on the sample thickness. If well separated echoes are present in the time trace a good approximation of d can be found by measuring the time delays between the reference and sample pulses Δt_{rs} and the sample and first echo pulses Δt_{se}:

$$d^* = \frac{c\Delta t_{rs}}{\bar{n} - 1}, \tag{6}$$

where the group refraction index over the THz spectral range $\bar{n}$ is

$$\bar{n} = \frac{1}{1 - 2\frac{\Delta t_{rs}}{\Delta t_{se}}}. \tag{7}$$

In general, if use of Eq. (6) is possible, one obtains a thickness value d^* that is more accurate than t, both reported in Table I. It is to be noted that d^* can be obtained only for the Si and LiF samples, for which some echoes are present in the time traces, but not for the A1 sample. In fact, due to its small thickness, low refraction index, and high absorption coefficient the THz pulse is totally superimposed with the first echo (see the inset of Fig. 1). In this case the echo truncation is not feasible, as well as the use of Eqs. (4) and (5). As Fig. 2 clearly shows, using these equations, when echoes are present in the time trace, always leads to the presence of the FP oscillations in the extracted optical parameters also for A1 for which the FP oscillations are apparently absent in the FFT amplitude (see Fig. 1). Moreover, if the sample pulse is superimposed on the first echo, one also has the drawback of the unavailability of a sample thickness determination.

The only way to determine the optical parameters as a function of frequency is to solve the implicit equation obtained by equating $\hat{T}_{\text{expt}}(\omega_j)$ with $\hat{T}(\hat{n},\omega_j)$ [Eq. (2)] in which the FP effects are self-contained. This equation can be solved only numerically. Defining

$$f(\hat{n},\omega) = \hat{T}_{\text{expt}}(\omega) - \frac{4\hat{n}}{(1+\hat{n})^2} \frac{e^{i(\hat{n}-1)\omega d/c}}{1 - \left(\frac{\hat{n}-1}{\hat{n}+1}\right)^2 e^{2i(\omega/c)\hat{n}d}}, \tag{8}$$

we have to find the $\hat{n}$ complex root that satisfies for each ω_j the equation $f(\hat{n},\omega_j) = 0$. One of the commonly considered approaches to solving root search problems is the NR method, but, as has been noted in the past, this method is unstable and its convergence is critical, especially when used with expressions containing rapidly oscillating functions such as Eq. (8). To overcome this problem, alternative methods based on minimization of error functions built using the theoretical and experimental transfer function were proposed [6]. However, all procedures based on this scheme revealed some application limits [11]. Furthermore, some of them require the implementation of particular algorithms especially when applied to data coming from thin samples. Ultimately, these approaches are unsuitable for nonspecialists in numerical computing.

The computational procedure proposed here to solve Eq. (8) is based on Davidenko's method in complex root search. It can be considered as a sort of Newton method applied to complex function root search problems [12]. The Davidenko method allows us to find the roots of complex functions by the numerical solution of a differential equation in place of the original equation. Further, convergence of the Davidenko method is in general faster than other methods and it does not need the initial value to be very close to the solution as in the NR method. One advantage of this method relies on the possibility to solve a differential equation by using a standard mathematical package.

Calling $\mathcal{D}(\hat{n}) = {}^{\partial f(\hat{n})}/_{\partial \hat{n}}$ the symbolic derivative of f with respect to $\hat{n}$ and introducing a dummy variable ξ in the functional dependence of $\hat{n}$,

$$\hat{n}(\xi) = n(\xi) + i\kappa(\xi),$$

it is necessary to solve the differential complex equation

$$\frac{\partial \hat{n}(\xi)}{\partial \xi} + \frac{f(\hat{n})\mathcal{D}(\hat{n})^*}{|\mathcal{D}(\hat{n})|^2} = 0. \tag{9}$$

Equation (9) can be split into a coupled real differential equation system

$$\frac{\partial n(\xi)}{\partial \xi} + \frac{\text{Re}[\mathcal{D}(\hat{n})]\text{Re}[f(\hat{n})] + \text{Im}[\mathcal{D}(\hat{n})]\text{Im}[f(\hat{n})]}{|\mathcal{D}(\hat{n})|^2} = 0,$$

$$\frac{\partial \kappa(\xi)}{\partial \xi} + \frac{\text{Re}[\mathcal{D}(\hat{n})]\text{Im}[f(\hat{n})] - \text{Re}[f(\hat{n})]\text{Im}[\mathcal{D}(\hat{n})]}{|\mathcal{D}(\hat{n})|^2} = 0$$

and the roots solution of Eq. (8) for each ω_j value are found asymptotically for $\xi \to \infty$: $\hat{n}(\infty) = n(\infty) + i\kappa(\infty)$.

In order to obtain the root values one has to solve the two coupled real differential equation system. It is convenient to solve this system numerically using standard mathematical packages that allow one to obtain the numerical solutions for a large enough ξ value within an acceptable computational time also on personal computers. In order to obtain a rapid convergence (small ξ interval) the initial root search values for the algorithm are found by using Eqs. (4) and (5).

As pointed out in previous studies, the minimization or complete removal of the residual Fabry-Perot oscillations present in the behaviors of the optical parameters is obtained by optimizing the sample thickness [10,11]. Indeed, up to now the sample thickness was considered the only parameter to be optimized for the extraction of the optical parameters in thin samples.

As can be noted from Fig. 1, all time-domain data present the zero line reference (ZLR) before the THz pulse. The time extension of the ZLR before the pulse is in general assumed to be constant over the course of the experimental session. However, experimental investigations carried out on our THz TDS system showed a drift in the ZLR up to more than 100 fs during the experimental sessions (lasting several hours). Tests carried out to clarify the origin of this drift showed that temperature variation of optical fibers was primarily responsible for this systematic error. As a consequence, the sample-reference delay time can be affected by this error, from now on called Δt_{instr}. This error is normally much smaller than the delay time between the THz reference and sample pulses and normally has a negligible effect on the calculation of $\hat{n}$ (see Fig. 1, panel Si or LiF). However, when thin and low-refraction-index samples have to be measured, such as in the case of the sample A1 (see Fig. 1), this variation becomes important and Δt_{instr} can be comparable to the true reference-sample delay time.

In order to recover the true spectral variation of $\hat{n}$ for the thinner sample A1 we have improved the signal extraction procedure by introducing a further adjustable parameter that takes account of Δt_{instr}. Considering that the Fourier transform of a pulse signal is by definition

$$\hat{E}(\omega) = \int p(t) e^{i\omega t} dt$$

and by introducing the Δt_{instr} parameter in an incorrect transfer function $\hat{T}'(\omega)$, we have

$$\begin{aligned}\hat{T}'(\omega) &= \frac{\int p_{\text{sample}}(t + \Delta t_{\text{instr}}) e^{i\omega t} dt}{\hat{E}_{\text{ref}}(\omega)} \\ &= \frac{\int p(\tilde{t}) e^{i\omega \tilde{t}} e^{-i\omega \Delta t_{\text{instr}}} d\tilde{t}}{\hat{E}_{\text{ref}}(\omega)} \\ &= \hat{T}(\omega) e^{-i\omega \Delta t_{\text{instr}}} \\ &= T(\omega) e^{i[\varphi(\omega) - \omega \Delta t_{\text{instr}}]}.\end{aligned}$$

Thus Δt_{instr} gives to $\hat{T}_{\text{expt}}(\omega_j)$ an extra phase-frequency-dependent contribution with respect to the true experimental transfer function. It should be noted that this correction can be implemented in a simple way in the computational procedure as an adjustable parameter of the original FFT data set $\hat{T}_{\text{expt}}(\omega_j)$, without involving a reprocessing of the time trace data and without a significant increase of computational time.

A typical computational run of our code on a 400 data array length spanning the available frequency range 0–4 THz of our apparatus takes about 10 s on a PC dated 2011 and about 4 s on a last generation PC, thus allowing us to perform in a reasonable time several runs in order to adjust at the best-fit parameter values.

The overall convergency relative error committed by the procedure can be estimated by considering the following expression:

$$\text{Conv Err} = \sum_j \left| \text{Re}\left[\frac{f(\hat{n}_j, \omega_j)}{\hat{T}_{\text{expt}}(\omega_j)} \right] \right| + \left| \text{Im}\left[\frac{f(\hat{n}_j, \omega_j)}{\hat{T}_{\text{expt}}(\omega_j)} \right] \right|.$$

The precision of our calculation for the refractive index and absorption coefficient is such that typical values for Conv Err obtained in our application are of the order 10^{-8}. That means that the relative difference, of the real or imaginary part, between any experimental and theoretical transfer function spectral component is in the worst case of the order 10^{-8}.

IV. RESULTS AND DISCUSSION

As a test of our computational procedure we applied it to the Si and LiF full time trace starting from the thickness values d^* obtained by means of Eq. (6). The thickness parameter was then adjusted to the final value d in order to reach the accurate cancellation of FP oscillations [7,8,10,11]. Results are shown in Fig. 2, where the accuracy of the FP oscillations removal from the optical parameters is evident. It should be noted that the time-windowed data treated by Eqs. (4) and (5) gave for Si and LiF the same results of the general method, so indicating the reliability of our algorithm.

Subsequently, we applied our procedure to the optically thin sample A1. Different from Si and LiF data processing, we found that in sample A1, to achieve the complete removal of the FP oscillations, it is necessary to adjust both the sample

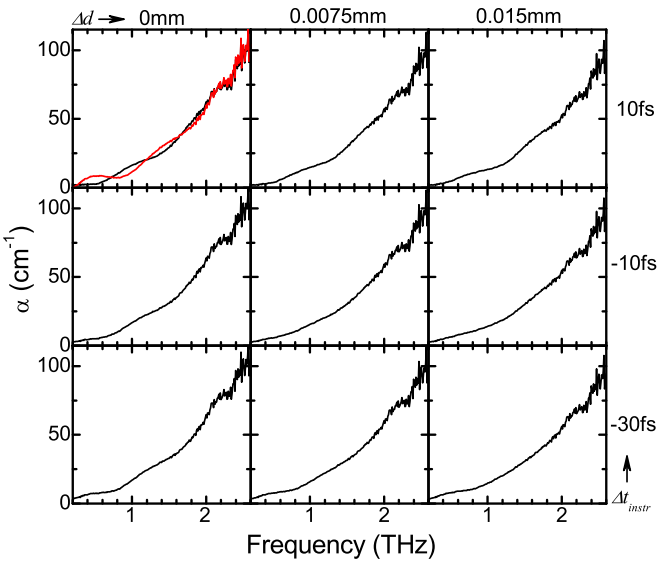

FIG. 3. Graphic-lattice form of the best parameter search performed on the sample A1 for the absorption coefficient. The best fit is reported in the central plot. In the top left plot the variation obtained by Eq. (5) [red (gray) line] is also shown for comparison.

thickness d and the Δt_{instr} parameters. A quadratic fit of the minimum THz pulse peaks has also been applied in order to enhance the time resolution for the determination of the sample-reference delay time.

We report in Fig. 3, in a graphic-lattice form, the optimized parameter search performed on the A1 absorption coefficient, where the plots in each row (column) have been carried out at constant (variable) Δt_{instr} and variable (constant) d. The central plot represents the best fit obtained by minimizing the FP oscillations according to the criteria given in Ref. [11]. As can be seen following the plots in the central column, if the Δt_{instr} parameter is not optimized, residual FP oscillations remain in the absorption coefficient frequency dependence. It is worthwhile to note that in the case of A1 this is really important in order to preserve the behavior of the spectroscopic features (i.e., the ω^2-like background in the range 0–2 THz [22,23] and the peak visible at about 2.1 THz [24]).

V. CONCLUSION

In this paper we have proposed a numerical procedure able to extract the optical parameters from THz TDS data in very thin samples. Like previous methods, our method works equally well with samples of varied thickness, refractive index, and absorption coefficient. In distinction from previous methods, we have shown that in order to obtain an accurate determination of the optical parameters in strongly absorbent optically thin samples it is necessary to take into account an instrumental systematic error that affects the pulse sample-reference delay time. Furthermore, we have shown that the correction of this error can be easily incorporated in a computationally efficient manner within a numerical procedure. This is essential in order to obtain the frequency dependence of the optical parameters without the uncertainty due to the FP oscillations. Such oscillations could in fact obscure or mask relevant spectroscopic information as shown in Fig. 3.

It is worthwhile to note that preliminary tests carried out to clarify the origin of this systematic error have shown that temperature variation of optical fibers could be the main cause of sample-reference delay time drifting. This suggests that this effect could be common to many THz TDS setups based on optical fibers. However, this effect could be present also in THz TDS setups without optical fibers due to electronic or thermal drift of different origin. Finally, our procedure is based on the direct application of a numerical method (the Davidenko method) which, in principle, can be implemented in personal computers using standard mathematical packages even by nonspecialists in numerical calculation.

For all these reasons the use of this procedure might therefore be of interest to a wide audience of researchers, especially when measurements have to be performed on very thin and strongly absorbent samples with refractive index close to 1, such as biological matter, water, solutions of biomolecules, or organic materials with hydrogen bonds such as carbohydrates (i.e., cellulose and its derivatives).

ACKNOWLEDGMENTS

This work was funded by the Ministero dell'Istruzione, dell'Università e della Ricerca (Progetto Premiale "THEIA"). R. M. Montereali and M. A. Vincenti are gratefully acknowledged for providing the colored LiF sample. Finally, we thank E. Del Re for his close reading of our manuscript.

[1] S. S. Dhillon *et al.*, J. Phys. D **50**, 043001 (2017).
[2] Y. Lee, *Principles of Terahertz Science and Technology* (Springer Science+Business Media, New York, 2009).
[3] P. U. Jepsen, D. G. Cooke, and M. Koch, Laser Photon. Rev. **5**, 124 (2011).
[4] J. B. Pendry, D. Schurig, and D. R. Smith, Science **312**, 1780 (2006).
[5] W. C. Chew, *Waves and Fields in Inhomogeneous Media* (Wiley-IEEE, Hoboken, 1999).
[6] L. Duvillaret, F. Garet, and J.-L. Coutaz, IEEE J. Sel. Top. Quantum Electron. **2**, 739 (1996).
[7] L. Duvillaret, F. Garet, and J.-L. Coutaz, Appl. Opt. **38**, 409 (1999).
[8] T. D. Dorney, R. G. Baraniuk, and D. M. Mittleman, J. Opt. Soc. Am. A **18**, 1562 (2001).
[9] P. U. Jepsen and B. M. Fischer, Opt. Lett. **30**, 29 (2005).
[10] I. Pupeza, R. Wilk, and M. Koch, Opt. Express **15**, 4335 (2007).
[11] M. Scheller, C. Jansen, and M. Koch, Opt. Commun. **282**, 1304 (2009).
[12] H. A. N. Hejase, IEEE Trans. Microwave Theory Tech. **41**, 141 (1993).
[13] R. Fastampa, M. Missori, M. C. Braidotti, C. Conti, M. A. Vincenti, and R. M. Montereali, Results Phys. **6**, 74 (2016).
[14] M. A. Vincenti, G. Baldacchini, V. S. Kalinov, R. M. Montereali, and A. P. Voitovich, IOP Conf. Ser. **15**, 012053 (2010).
[15] M. Missori, M. Righini, and S. Selci, Opt. Commun. **231**, 99 (2004).
[16] A. M. Conte, O. Pulci, A. Knapik, J. Bagniuk, R. D. Sole, J. Łojewska, and M. Missori, Phys. Rev. Lett. **108**, 158301 (2012).
[17] C. Corsaro, D. Mallamace, J. Łojewska, F. Mallamace, L. Pietronero, and M. Missori, Sci. Rep. **3**, 2896 (2013).
[18] A. M. Conte, O. Pulci, M. C. Misiti, J. Łojewska, L. Teodonio, C. Violante, and M. Missori, Appl. Phys. Lett. **104**, 224101 (2014).
[19] C. Corsaro, D. Mallamace, S. Vasi, L. Pietronero, F. Mallamace, and M. Missori, Phys. Chem. Chem. Phys. **18**, 33335 (2016).
[20] M. Missori, O. Pulci, L. Teodonio, C. Violante, I. Kupchak, J. Bagniuk, J. Łojewska, and A. M. Conte, Phys. Rev. B **89**, 054201 (2014).
[21] M. Franz, B. M. Fischer, and M. Walther, Appl. Phys. Lett. **92**, 021107 (2008).
[22] U. Strom and P. C. Taylor, Phys. Rev. B **16**, 5512 (1977).
[23] M. Naftaly and R. E. Miles, Proc. IEEE **95**, 1658 (2007).
[24] F. S. Vieira and C. Pasquini, Anal. Chem. **86**, 3780 (2014).